

Effects of the Amino Acid Linkers on the Melanoma-Targeting and Pharmacokinetic Properties of ^{111}In -Labeled Lactam Bridge–Cyclized α -MSH Peptides

Haixun Guo¹, Jianquan Yang¹, Fabio Gallazzi², and Yubin Miao^{1,3,4}

¹College of Pharmacy, University of New Mexico, Albuquerque, New Mexico; ²Department of Biochemistry, University of Missouri, Columbia, Missouri; ³Cancer Research and Treatment Center, University of New Mexico, Albuquerque, New Mexico; and

⁴Department of Dermatology, University of New Mexico, Albuquerque, New Mexico

The purpose of this study was to examine the profound effects of the amino acid linkers on the melanoma-targeting and pharmacokinetic properties of ^{111}In -labeled lactam bridge–cyclized DOTA-[X]-CycMSH_{hex} {1,4,7,10-tetraazacyclododecane-1,4,7,10-tetraacetic acid-[X]-c[Asp-His-DPhe-Arg-Trp-Lys]-CONH₂; X = GGNle, GENle, or NleGE; GG = -Gly-Gly- and GE = -Gly-Glu-} peptides. **Methods:** Three novel peptides (DOTA-GGNle-CycMSH_{hex}, DOTA-GENle-CycMSH_{hex}, and DOTA-NleGE-CycMSH_{hex}) were designed and synthesized. The melanocortin-1 (MC1) receptor-binding affinities of the peptides were determined in B16/F1 melanoma cells. The melanoma-targeting and pharmacokinetic properties of ^{111}In -DOTA-GGNle-CycMSH_{hex} and ^{111}In -DOTA-GENle-CycMSH_{hex} were determined in B16/F1 melanoma-bearing C57 mice. **Results:** DOTA-GGNle-CycMSH_{hex} and DOTA-GENle-CycMSH_{hex} displayed 2.1 and 11.5 nM MC1 receptor-binding affinities, whereas DOTA-NleGE-CycMSH_{hex} showed 873.4 nM MC1 receptor-binding affinity. The introduction of the -GG- linker maintained high melanoma uptake while decreasing kidney and liver uptake of ^{111}In -DOTA-GGNle-CycMSH_{hex}. The tumor uptake of ^{111}In -DOTA-GGNle-CycMSH_{hex} was 19.05 ± 5.04 and 18.6 ± 3.56 percentage injected dose per gram at 2 and 4 h after injection, respectively. ^{111}In -DOTA-GGNle-CycMSH_{hex} exhibited 28%, 32%, and 42% less kidney uptake than ^{111}In -DOTA-Nle-CycMSH_{hex} we reported previously, and 61%, 65%, and 68% less liver uptake than ^{111}In -DOTA-Nle-CycMSH_{hex} at 2, 4, and 24 h after injection, respectively. **Conclusion:** The amino acid linkers exhibited profound effects on the melanoma-targeting and pharmacokinetic properties of the ^{111}In -labeled lactam bridge–cyclized α -melanocyte-stimulating hormone peptides. Introduction of the -GG- linker maintained high melanoma uptake while reducing kidney and liver uptake of ^{111}In -DOTA-GGNle-CycMSH_{hex}, highlighting its potential as an effective imaging probe for melanoma detection, as well as a therapeutic peptide for melanoma treatment when labeled with a therapeutic radionuclide.

Key Words: alpha-melanocyte stimulating hormone; radiolabeled cyclic peptide; melanoma imaging

J Nucl Med 2011; 52:608–616

DOI: 10.2967/jnumed.110.086009

Over the last decade, both radiolabeled linear and cyclized α -melanocyte-stimulating hormone (α -MSH) peptides have been designed to target G protein-coupled melanocortin-1 (MC1) receptors (1–5) for melanoma radioimaging and radiotherapy (6–20). Because of the stabilization of secondary structures (i.e., β -turns), the cyclic peptides possess less conformational freedom and higher stability than the linear peptides. Furthermore, the stabilization of secondary structures makes the cyclic peptides better fit the receptor-binding pocket, thus enhancing their receptor-binding affinities. Presently, disulfide bond, metal, and lactam bridge have been successfully used to cyclize the radiolabeled α -MSH peptides (9–13,15–20). Among these cyclization strategies, metal and lactam bridge cyclization resulted in greater tumor uptake and lower kidney uptake of the radiolabeled α -MSH peptides than the disulfide bridge cyclization (12,13,15–20).

We have successfully developed a class of ^{111}In -labeled lactam bridge–cyclized DOTA-conjugated α -MSH peptides for primary and metastatic melanoma detection (15–19). Initially, a Lys-Asp lactam bridge was used to cyclize the MC1 receptor-binding motif (His-DPhe-Arg-Trp) to yield a 12-amino acid cyclic α -MSH peptide {CycMSH: c[Lys-Nle-Glu-His-DPhe-Arg-Trp-Gly-Arg-Pro-Val-Asp]}. DOTA was conjugated to the N terminus of the CycMSH with or without an amino acid linker (-Gly-Glu- [GE]) for radiolabeling. ^{111}In -DOTA-GlyGlu-CycMSH displayed high melanoma uptake (10.40 ± 1.40 percentage injected dose [% ID]/g at 2 h after injection) in B16/F1 melanoma-bearing C57 mice (15). When ^{111}In -DOTA-GlyGlu-CycMSH was used as an imaging probe, both flank primary and pulmonary metastatic melanoma lesions could be clearly visualized by small-animal SPECT/CT (15,16).

Received Nov. 30, 2010; revision accepted Jan. 12, 2011.

For correspondence or reprints contact: Yubin Miao, 2502 Marble NE, MSC09 5360, College of Pharmacy, University of New Mexico, Albuquerque, NM 87131.

E-mail: ymiao@salud.unm.edu

COPYRIGHT © 2011 by the Society of Nuclear Medicine, Inc.

Recently, we identified another DOTA-conjugated lactam bridge-cyclized α -MSH peptide with a 6-amino acid peptide ring {DOTA-Nle-CycMSH_{hex}: DOTA-Nle-c[Asp-His-DPhe-Arg-Trp-Lys]-CONH₂} for melanoma targeting. The receptor-binding motif of His-DPhe-Arg-Trp was directly cyclized by an Asp-Lys lactam bridge. Interestingly, reduction of the ring size dramatically enhanced melanoma uptake (19.39 ± 1.65 %ID/g at 2 h after injection) and reduced kidney uptake (9.52 ± 0.44 %ID/g at 2 h after injection) of ¹¹¹In-DOTA-Nle-CycMSH_{hex}, compared with ¹¹¹In-DOTA-GlyGlu-CycMSH_{hex}, in B16/F1 melanoma-bearing C57 mice (15,19).

Hydrocarbon, amino acid, and polyethylene glycol linkers displayed profound favorable effects on the receptor-binding affinities and pharmacokinetics of radiolabeled bombesin (21–25), RGD (26–29), and α -MSH peptides (15,16). To examine the effects of the amino acid linkers on melanoma-targeting and pharmacokinetic properties, we designed 3 novel DOTA-conjugated lactam bridge-cyclized CycMSH_{hex} peptides with different amino acid linkers in this study based on the unique structure of DOTA-Nle-CycMSH_{hex} we previously reported (19). A neutral -Gly-Gly- (GG) linker and a negatively charged -GE-linker were inserted between the DOTA and Nle to generate DOTA-GGNle-CycMSH_{hex} and DOTA-GENle-CycMSH_{hex}. Furthermore, the negatively charged -GE-linker was introduced between Nle and CycMSH_{hex} to yield DOTA-NleGE-CycMSH_{hex}. The MC1 receptor-binding affinities of these 3 peptides were determined in B16/F1 melanoma cells. Only DOTA-GGNle-CycMSH_{hex} and DOTA-GENle-CycMSH_{hex} displayed low-nanomolar MC1 receptor-binding affinities. Hence, we further determined the melanoma-targeting and pharmacokinetic properties of ¹¹¹In-DOTA-GGNle-CycMSH_{hex} and ¹¹¹In-DOTA-GENle-CycMSH_{hex} in B16/F1 melanoma-bearing C57 mice.

MATERIALS AND METHODS

Chemicals and Reagents

Amino acids and resin were purchased from Advanced Chem-Tech Inc. and Novabiochem. DOTA-tri-*t*-butyl ester was purchased from Macrocylics Inc. for peptide synthesis. ¹²⁵I-Tyr²-[Nle⁴, DPhe⁷]- α -MSH (NDP-MSH) was obtained from PerkinElmer, Inc. for in vitro receptor-binding assay. ¹¹¹InCl₃ was purchased from MDS Nordion, Inc., for radiolabeling. All other chemicals used in this study were purchased from Thermo Fischer Scientific and used without further purification. B16/F1 murine melanoma cells were obtained from American Type Culture Collection.

Peptide Synthesis

New DOTA-GGNle-CycMSH_{hex}, DOTA-GENle-CycMSH_{hex}, and DOTA-NleGE-CycMSH_{hex} peptides were synthesized using standard fluorenylmethyloxycarbonyl chemistry according to our published procedure (19) with modifications. Briefly, linear peptide backbones of (tBu)₃DOTA-GGNle-Asp(O-2-PhiPr)-His(Trt)-DPhe-Arg(Pbf)-Trp(Boc)-Lys(Dde), (tBu)₃DOTA-GE(OtBu)-Nle-Asp(O-2-PhiPr)-His(Trt)-DPhe-Arg(Pbf)-Trp(Boc)-Lys(Dde), and (tBu)₃DOTA-NleGE(OtBu)-Asp(O-2-PhiPr)-His(Trt)-DPhe-Arg(Pbf)-Trp(Boc)-Lys(Dde) were synthesized on Sieber Amide resin by an Advanced ChemTech multiple-peptide synthesizer. Seventy

micromoles of resin, 210 μ mol of each fluorenylmethyloxycarbonyl-protected amino acid, and 210 μ mol of (tBu)₃DOTA were used for the synthesis. The protecting group of Dde was removed by 2% hydrazine for peptide cyclization. The protecting group of 2-phenylisopropyl was removed, and the protected peptide was cleaved from the resin through treatment with a mixture of 2.5% of trifluoroacetic acid and 5% of triisopropylsilane. After the precipitation with ice-cold ether and characterization by liquid chromatography-mass spectroscopy, each protected peptide was dissolved in H₂O/CH₃CN (50:50) and lyophilized to remove the reagents. Then, each protected peptide was further cyclized by coupling the carboxylic group from the Asp with the ϵ -amino group from the Lys. The cyclization reaction was achieved by an overnight reaction in dimethylformamide using benzotriazole-1-yl-oxy-tris-pyrrolidinophosphonium-hexafluorophosphate as a coupling agent in the presence of *N,N*-diisopropylethylamine. After the characterization by liquid chromatography-mass spectroscopy, each cyclized protected peptide was dissolved in H₂O/CH₃CN (50:50) and lyophilized to remove the reagents. The protecting groups were totally removed by treatment with a mixture of trifluoroacetic acid, thioanisole, phenol, water, ethanedithiol, and triisopropylsilane (87.5:2.5:2.5:2.5:2.5:2.5) for 2 h at room temperature (25°C). Each peptide was precipitated and washed with ice-cold ether 4 times, purified by reverse-phase high-performance liquid chromatography (RP-HPLC), and characterized by liquid chromatography-mass spectroscopy.

In Vitro Receptor-Binding Assay

The receptor-binding affinities (inhibitory concentration of 50% [IC₅₀]) of DOTA-GGNle-CycMSH_{hex}, DOTA-GENle-CycMSH_{hex}, and DOTA-NleGE-CycMSH_{hex} were determined by

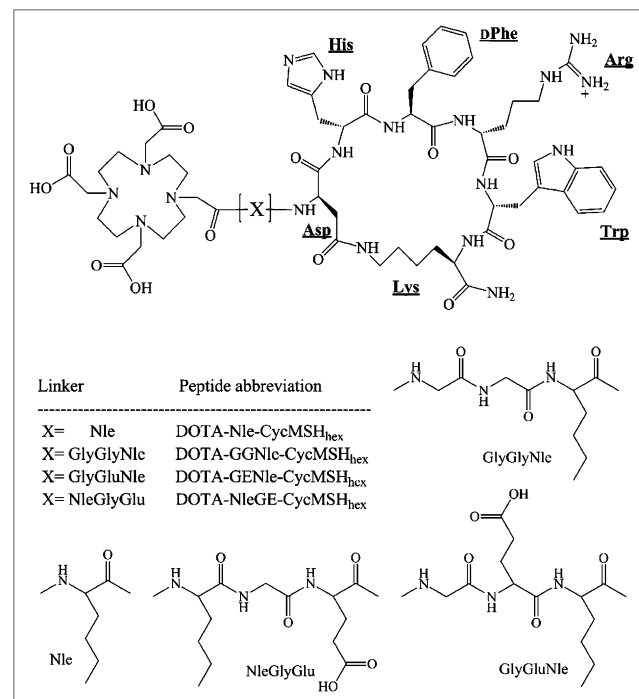


FIGURE 1. Structures of DOTA-Nle-CycMSH_{hex}, DOTA-GGNle-CycMSH_{hex}, DOTA-GENle-CycMSH_{hex}, and DOTA-NleGE-CycMSH_{hex}. Structure of DOTA-Nle-CycMSH_{hex} was cited from reference 19 for comparison.

an in vitro competitive binding assay according to our published procedure (19), with modifications. B16/F1 cells in 24-well cell culture plates (5×10^5 cells per well) were incubated at room temperature (25°C) for 2 h with approximately 60,000 cpm of ^{125}I -Tyr²-NDP-MSH in the presence of a 10^{-12} to 10^{-5} M concentration of each peptide in 0.3 mL of binding medium {Dulbecco's modified Eagle's medium with 25 mM *N*-(2-hydroxyethyl)-piperazine-*N'*-(2-ethanesulfonic acid), pH 7.4, 0.2% bovine serum albumin, 0.3 mM 1,10-phenanthroline}. The medium was aspirated after the incubation. The cells were rinsed twice with 0.5 mL of ice-cold 0.2% bovine serum albumin (pH 7.4)/0.01 M phosphate-buffered saline and lysed in 0.5 mL of 1N NaOH for 5 min. The activities associated with cells were measured in a Wallac 1480 automated γ -counter (PerkinElmer). The IC₅₀ of each peptide was calculated using Prism software (GraphPad Software).

Peptide Radiolabeling with ^{111}In

Since DOTA-NleGE-CycMSH_{hex} exhibited at least 78-fold lower receptor-binding affinity than DOTA-GGNle-CycMSH_{hex} and DOTA-GENle-CycMSH_{hex}, we only further evaluated DOTA-GGNle-CycMSH_{hex} and DOTA-GENle-CycMSH_{hex}. ^{111}In -DOTA-GGNle-CycMSH_{hex} and ^{111}In -DOTA-GENle-CycMSH_{hex} were prepared in a 0.5 M NH₄OAc-buffered solution at pH 4.5 according to our published procedure (19). Briefly, 50 μL of $^{111}\text{InCl}_3$ (37–74 MBq in 0.05 M HCl aqueous solution), 10 μL of a 1 mg/mL peptide aqueous solution, and 400 μL of 0.5 M NH₄OAc (pH 4.5) were added to a reaction vial and incubated at 75°C for 45 min. After the incubation, 10 μL of 0.5% ethylenediaminetetraacetic acid aqueous solution were added to the reaction vial to scavenge potential unbound $^{111}\text{In}^{3+}$ ions. The radiolabeled complexes were purified to a single species by Waters RP-HPLC on a Grace Vydac C-18 reverse-phase analytic column using the following gradient at a 1 mL/min flow rate. The mobile phase consisted of solvent A (20 mM HCl aqueous solution) and solvent B (100% CH₃CN). The gradient was initiated and kept at 82:18 A/B for 3 min followed by a linear gradient of 82:18 A/B to 72:28 A/B over 20 min. Then, the gradient was changed from 72:28 A/B to 10:90 A/B over 3 min followed by an additional 5 min at 10:90 A/B. Thereafter, the gradient was changed from 10:90 A/B to 82:18 A/B over 3 min. Each purified peptide sample was purged with N₂ gas for 20 min to remove the acetonitrile. The pH of the final solution was adjusted to 7.4 with 0.1 N NaOH and sterile saline for animal studies. The in vitro serum stability of ^{111}In -DOTA-GGNle-CycMSH_{hex} and ^{111}In -DOTA-GENle-CycMSH_{hex} was determined by incubation in mouse serum at 37°C for 24 h and monitored for degradation by RP-HPLC.

Biodistribution Studies

All animal studies were conducted with the approval of the Institutional Animal Care and Use Committee. The pharmacokinetics of ^{111}In -DOTA-GGNle-CycMSH_{hex} and ^{111}In -DOTA-GENle-CycMSH_{hex} were determined in B16/F1 melanoma-bearing C57 female mice (Harlan). Each C57 mouse was subcutaneously inoculated with 1×10^6 B16/F1 cells in the right flank to generate B16/F1 melanoma. Ten days after inoculation, the tumor weights reached approximately 0.2 g. Each melanoma-bearing mouse was injected with 0.037 MBq of ^{111}In -DOTA-GGNle-CycMSH_{hex} or ^{111}In -DOTA-GENle-CycMSH_{hex} via the tail vein. Groups of 5 mice were sacrificed at 0.5, 2, 4, and 24 h after injection, and tumors and organs of interest were harvested, weighed, and counted. Blood values were taken as 6.5% of the whole-body weight. The specificities of tumor uptake of ^{111}In -DOTA-GGNle-CycMSH_{hex} and ^{111}In -

DOTA-GENle-CycMSH_{hex} were determined by coinjecting 10 μg (6.07 nmol) of unlabeled NDP-MSH, which is a linear α -MSH peptide analog with picomolar MC1 receptor-binding affinity.

Melanoma Imaging

Since ^{111}In -DOTA-GGNle-CycMSH_{hex} displayed more favorable tumor targeting and pharmacokinetic properties than ^{111}In -DOTA-GENle-CycMSH_{hex}, we only further evaluated the melanoma imaging property of ^{111}In -DOTA-GGNle-CycMSH_{hex}. One B16/F1 melanoma-bearing C57 mouse (10 d after cell inoculation) was injected with 14.8 MBq of ^{111}In -DOTA-GGNle-CycMSH_{hex} via the tail vein. The mouse was sacrificed for small-animal SPECT/CT (Nano-SPECT/CT; BioScan) imaging at 2 h after injection. The CT was immediately followed by the whole-body SPECT. SPECT scans of 24 projections were acquired. Reconstructed SPECT and CT data were visualized and coregistered using InVivoScope (BioScan).

Metabolites of ^{111}In -DOTA-GGNle-CycMSH_{hex} in Melanoma and Urine

From the mouse used for SPECT/CT, both melanoma and urine were collected for analyses of ^{111}In -DOTA-GGNle-CycMSH_{hex} metabolites. The tumor was homogenized for 5 min. An equal volume of ethanol was added to the tumor sample. The tumor sample was stirred in a vortex mixer and then centrifuged at 16,000g for 5 min. The supernatant was transferred to a glass test tube and purged with N₂ gas for 20 min to remove the ethanol. Aliquots of the supernatant were injected into the HPLC. The urinary sample was directly centrifuged at 16,000g for 5 min before the HPLC analysis. Thereafter, aliquots of the urine were injected into the HPLC. The HPLC gradient already described was used for the analyses of metabolites.

Statistical Analysis

Statistical analysis was performed using the Student *t* test for unpaired data. A 95% confidence level was chosen to determine the significance of differences in tumor and kidney uptake between ^{111}In -DOTA-GGNle-CycMSH_{hex} and ^{111}In -DOTA-GENle-CycMSH_{hex}, as well as the significance of differences in tumor and kidney uptake in ^{111}In -DOTA-GGNle-CycMSH_{hex} or ^{111}In -DOTA-GENle-CycMSH_{hex} with and without NDP-MSH coinjection. Differences at the 95% confidence level ($P < 0.05$) were considered significant.

RESULTS

Three α -MSH peptides—DOTA-GGNle-CycMSH_{hex}, DOTA-GENle-CycMSH_{hex}, and DOTA-NleGE-CycMSH_{hex}—were synthesized and purified by HPLC. All 3 peptides displayed greater than 95% purity after HPLC purification. The schematic structures of the peptides are shown in Figure 1. The identities of the peptides were confirmed by electrospray ionization mass spectrometry. The calculated and found molecular weights of the peptides are presented in Table 1. The receptor-binding affinities of the peptides were determined in B16/F1 melanoma cells. The IC₅₀ values of DOTA-GGNle-CycMSH_{hex}, DOTA-GENle-CycMSH_{hex}, and DOTA-NleGE-CycMSH_{hex} were 2.1, 11.5, and 873.4 nM in B16/F1 cells, respectively (Table 1; Fig. 2).

We further evaluated only DOTA-GGNle-CycMSH_{hex} and DOTA-GENle-CycMSH_{hex} because both peptides displayed low-nanomolar MC1 receptor-binding affinities. The pep-

tides were readily labeled with ^{111}In in 0.5 M ammonium acetate solution at pH 4.5 with greater than 95% radiolabeling yield. Each ^{111}In -labeled peptide was completely separated from its excess nonlabeled peptide by RP-HPLC. The retention times of the peptides and their ^{111}In -labeled conjugates are shown in Table 1. The retention times of ^{111}In -DOTA-GGNle-CycMSH_{hex} and ^{111}In -DOTA-GENle-CycMSH_{hex} were 17.7 and 21.7 min, respectively. They showed greater than 98% radiochemical purity after HPLC purification and were stable in mouse serum at 37°C for 24 h. Only intact ^{111}In -labeled conjugates were detected by RP-HPLC after 24 h of incubation in mouse serum.

We further evaluated the melanoma-targeting and pharmacokinetic properties of ^{111}In -DOTA-GGNle-CycMSH_{hex} and ^{111}In -DOTA-GENle-CycMSH_{hex} in B16/F1 melanoma-bearing C57 mice. The biodistribution results are shown in Table 2. ^{111}In -DOTA-GGNle-CycMSH_{hex} exhibited rapid, high melanoma uptake and prolonged tumor retention. The tumor uptake of ^{111}In -DOTA-GGNle-CycMSH_{hex} was 18.39 ± 2.22 %ID/g at 0.5 h after injection and peaked at 19.05 ± 5.04 %ID/g at 2 h after injection. ^{111}In -DOTA-GGNle-CycMSH_{hex} displayed similar high tumor uptake (18.6 ± 3.56 %ID/g) at 4 h after injection. Even at 24 h after injection, 6.77 ± 0.84 %ID/g of ^{111}In -DOTA-GGNle-CycMSH_{hex} activity remained in the tumor. Approximately 98% of the tumor uptake of ^{111}In -DOTA-GGNle-CycMSH_{hex} was blocked by 10 μg (6.07 nmol) of nonradiolabeled NDP-MSH ($P < 0.05$), demonstrating that the tumor uptake was specific and MC1 receptor-mediated. Whole-body clearance of ^{111}In -DOTA-GGNle-CycMSH_{hex} was rapid, with approximately 88.4% of the injected radioactivity cleared through the urinary system by 2 h after injection. Normal-organ uptake of ^{111}In -DOTA-GGNle-CycMSH_{hex} was low (<1.31 %ID/g), except for the kidneys at 2, 4, and 24 h after injection. Liver uptake of ^{111}In -DOTA-GGNle-CycMSH_{hex} was less than 0.61 %ID/g at 2 h after injection. Kidney uptake was 15.19 ± 2.75 %ID/g at 0.5 h after injection and decreased to 6.84 ± 0.92 %ID/g at 2 h after injection. Coinjection of NDP-MSH did not significantly reduce kidney uptake of the ^{111}In -DOTA-GGNle-CycMSH_{hex} activity at 2 h af-

ter injection, indicating that kidney uptake was not MC1 receptor-mediated. High tumor uptake and prolonged tumor retention coupled with rapid whole-body clearance resulted in high ratios of tumor-to-blood uptake and tumor-to-normal-organ uptake as early as 0.5 h after injection. The ratios of tumor-to-liver uptake for ^{111}In -DOTA-GGNle-CycMSH_{hex} were 33.42 and 31.0 at 2 and 4 h, after injection, respectively, whereas the ratios of tumor-to-kidney uptake for ^{111}In -DOTA-GGNle-CycMSH_{hex} were 2.79 and 2.73 at 2 and 4 h after injection, respectively.

As we anticipated, ^{111}In -DOTA-GENle-CycMSH_{hex} showed lower tumor uptake than ^{111}In -DOTA-GGNle-CycMSH_{hex} at 0.5, 2, and 4 h after injection. Tumor uptake of ^{111}In -DOTA-GENle-CycMSH_{hex} was 2, 2.5, and 3 times that of ^{111}In -DOTA-GENle-CycMSH_{hex} at 0.5, 2, and 4 h after injection, respectively (Table 2). Coinjection of nonradioactive NDP-MSH blocked 95.6% of tumor uptake at 2 h after injection ($P < 0.05$), indicating that tumor uptake of ^{111}In -DOTA-GENle-CycMSH_{hex} was MC1 receptor-specific. Despite the fact that kidney uptake of ^{111}In -DOTA-GENle-CycMSH_{hex} was similar to that of ^{111}In -DOTA-GGNle-CycMSH_{hex} at 2, 4, and 24 h after injection, ^{111}In -DOTA-GENle-CycMSH_{hex} showed 40% lower kidney uptake than ^{111}In -DOTA-GGNle-CycMSH_{hex} at 0.5 h after injection ($P < 0.05$). Kidney uptake of ^{111}In -DOTA-GENle-CycMSH_{hex} was as low as 9.06 ± 2.20 %ID/g at 0.5 h after injection and decreased to 5.54 ± 0.63 %ID/g at 2 h after injection.

We further evaluated the melanoma-imaging properties of ^{111}In -DOTA-GGNle-CycMSH_{hex}, because it showed more favorable biodistribution properties than ^{111}In -DOTA-GENle-CycMSH_{hex}. The whole-body SPECT/CT images are presented in Figure 3. Flank melanoma tumors were clearly visualized by SPECT/CT using ^{111}In -DOTA-GGNle-CycMSH_{hex} as an imaging probe. The whole-body images showed high ratios of tumor-to-normal-organ uptake except for the kidneys, as was consistent with the biodistribution results. Melanoma and urinary metabolites of ^{111}In -DOTA-GGNle-CycMSH_{hex} were analyzed by RP-HPLC at 2 h after injection. Figure 4 illustrates the HPLC profiles for both melanoma and urine samples. ^{111}In -

TABLE 1
DOTA-Conjugated Lactam Bridge-Cyclized α -MSH Peptides

Parameter	DOTA-Nle-CycMSH _{hex}	DOTA-GGNle-CycMSH _{hex}	DOTA-GENle-CycMSH _{hex}	DOTA-NleGE-CycMSH _{hex}
Amino acid linker between DOTA and cyclic peptide moiety	-Nle-	-GGNle-	-GENle-	-NleGE-
Calculated molecular weight (Da)	1,368.5	1,482.6	1,554.6	1,554.6
Found molecular weight (Da)	1,368.2	1,482.0	1,554.0	1,554.0
Molecular formula	C ₆₄ H ₉₃ N ₁₉ O ₁₅	C ₆₈ H ₉₉ N ₂₁ O ₁₇	C ₇₁ H ₁₀₃ N ₂₁ O ₁₉	C ₇₁ H ₁₀₃ N ₂₁ O ₁₉
MC1 receptor binding affinity (nM)	1.8	2.1	11.5	873.4
HPLC retention time (min)	14.3	14.8	15.4	9.6
HPLC retention time for ^{111}In -conjugate (min)	10.7	17.7	21.7	NA

NA = not applicable.

Data of DOTA-Nle-CycMSH_{hex} were cited from reference 19 for comparison.

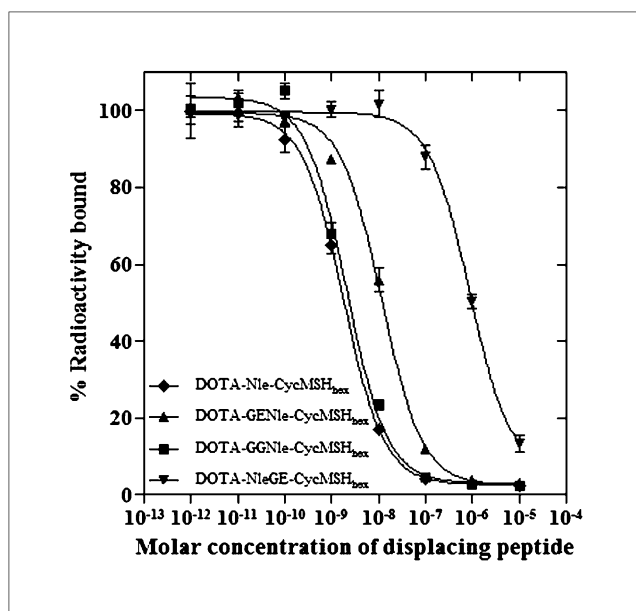


FIGURE 2. In vitro competitive binding curves of DOTA-Nle-CycMSH_{hex}, DOTA-GGNle-CycMSH_{hex}, DOTA-GENle-CycMSH_{hex}, and DOTA-NleGE-CycMSH_{hex} in B16/F1 melanoma cells. IC₅₀ values of DOTA-Nle-CycMSH_{hex}, DOTA-GGNle-CycMSH_{hex}, DOTA-GENle-CycMSH_{hex}, and DOTA-NleGE-CycMSH_{hex} were 1.8, 2.1, 11.5, and 873.4 nM, respectively. Data of DOTA-Nle-CycMSH_{hex} were cited from reference 19 for comparison.

DOTA-GGNle-CycMSH_{hex} remained intact in both tumor and urine 2 h after injection (Fig. 4).

DISCUSSION

We have been interested in developing lactam bridge-cyclized α -MSH peptides to target the MC1 receptors for melanoma detection (15–19). Unique lactam bridge cyclization makes the cyclic α -MSH peptides resistant to proteolytic degradation in vivo and provides the flexibility for fine structural modification (15,17,19). Recently, we identified ¹¹¹In-DOTA-Nle-CycMSH_{hex} with a 6-amino acid ring targeting the MC1 receptors for melanoma imaging (19). Among these reported ¹¹¹In-labeled lactam bridge-cyclized α -MSH peptides (15,17,19), ¹¹¹In-DOTA-Nle-CycMSH_{hex} displayed the highest melanoma uptake (24.94 ± 4.58 %ID/g at 0.5 h after injection and 19.39 ± 1.65 %ID/g at 2 h after injection) in B16/F1 melanoma-bearing mice (19). Reduction of the ring size improved tumor uptake and reduced kidney uptake of ¹¹¹In-DOTA-Nle-CycMSH_{hex}, providing new insight into the design of lactam bridge-cyclized α -MSH peptides for melanoma targeting.

Hydrocarbon, amino acid, and polyethylene glycol linkers have been used to optimize the receptor-binding affinities and modify the pharmacokinetic properties of radiolabeled bombesin (21–25), RGD (26–29), and α -MSH peptides (15,16). For instance, Hoffman et al. reported that the hydrocarbon linkers ranging from 5-carbon to 8-carbon between the DOTA and bombesin peptide resulted in 0.6–1.7 nM receptor-binding affinities for the DOTA-conjugated bombesin peptides. Either

shorter or longer hydrocarbon linkers dramatically reduce the receptor-binding affinity by 100-fold (21). Parry et al. reported the profound effects of amino acid linkers (-Gly-Gly-Gly-, -Gly-Ser-Gly-, -Gly-Ser-Ser-, and -Gly-Glu-Gly-) between the DOTA and bombesin peptide on tumor and normal-organ uptake of the radiolabeled peptides (25). ⁶⁴Cu-labeled DOTA-conjugated bombesin peptide with the -Gly-Gly-Gly- linker displayed higher PC-3 tumor uptake, whereas the -Gly-Ser-Gly- linker resulted in lower kidney uptake (25). Recently, the group led by Liu reported an improvement in the tumor uptake and pharmacokinetics of ⁶⁴Cu- and ^{99m}Tc-labeled cyclic RGD peptides using the -Gly-Gly-Gly- and polyethylene glycol 4 (PEG₄) linkers (26–29). We also demonstrated that the introduction of a negatively charged -GE- linker enhanced melanoma uptake and reduced kidney uptake of ¹¹¹In-DOTA-GlyGlu-CycMSH, compared with ¹¹¹In-DOTA-CycMSH (15). Hence, we evaluated the effects of -GG- and -GE- linkers on the melanoma-targeting and pharmacokinetic properties of ¹¹¹In-DOTA-[X]-CycMSH_{hex} peptide constructs in this study.

DOTA-Nle-CycMSH_{hex} displayed 1.8 nM MC1 receptor-binding affinity in B16/F1 melanoma cells in our previous report (19). The MC1 receptor-binding sequence of His-DPhe-Arg-Trp was directly cyclized by an Asp-Lys lactam bridge to generate the CycMSH_{hex} moiety. The radiometal chelator DOTA was conjugated to the CycMSH_{hex} moiety via an Nle to form DOTA-Nle-CycMSH_{hex} peptide. Based on the unique structure of DOTA-Nle-CycMSH_{hex}, we initially introduced the amino acid linker (-GE-) between the DOTA and Nle or between the Nle and CycMSH_{hex} moiety to determine which position was suitable for an amino acid linker. We found that the moiety of Nle-CycMSH_{hex} was critical for maintaining the low-nanomolar MC1 receptor-binding affinity of the peptide. The introduction of the -GE- linker between the Nle and CycMSH_{hex} moiety dramatically reduced the MC1 receptor-binding affinity to 873.4 nM, whereas the introduction of the -GE- linker between the DOTA and Nle decreased the MC1 receptor-binding affinity only to 11.5 nM. Interestingly, the -GG- linker between the DOTA and Nle maintained the MC1 receptor-binding affinity at 2.1 nM, further indicating that the moiety of Nle-CycMSH_{hex} played a crucial role in maintaining the low-nanomolar MC1 receptor-binding affinity of the peptide. Furthermore, the amino acid between the DOTA and the moiety of Nle-CycMSH_{hex} also showed a significant impact on the MC1 receptor-binding affinity of the peptide. The neutral -GG- linker was better than the negatively charged -GE- linker in maintaining the low-nanomolar MC1 receptor-binding affinity of the peptide. The IC₅₀ value of DOTA-GENle-CycMSH_{hex} was 5.5 times that of DOTA-GGNle-CycMSH_{hex}. It was likely that the electrostatic interaction between the negatively charged Glu in the -GE- linker and the positively charged Arg in the moiety of Nle-CycMSH_{hex} affected the configuration of the MC1 receptor-binding region (His-DPhe-Arg-Trp). The difference in MC1 receptor-binding affinity between DOTA-GGNle-CycMSH_{hex} and DOTA-GENle-CycMSH_{hex} (2.1 nM vs. 11.5 nM) was also

TABLE 2
Biodistribution of ¹¹¹In-DOTA-GGNle-CycMSH_{hex} and ¹¹¹In-DOTA-GENle-CycMSH_{hex} in B16/F1 Melanoma-Bearing C57 Mice

Tissue	¹¹¹ In-DOTA-GGNle-CycMSH _{hex}				¹¹¹ In-DOTA-GENle-CycMSH _{hex}			
	0.5 h	2 h	4 h	24 h	0.5 h	2 h	4 h	24 h
%ID/g								
Tumor	18.39 ± 2.22	19.05 ± 5.04	18.6 ± 3.56	6.77 ± 0.84	11.75 ± 2.00*	8.99 ± 1.91*	5.3 ± 2.84*	4.40 ± 0.87*
Brain	0.21 ± 0.18	0.03 ± 0.03	0.04 ± 0.03	0.01 ± 0.01	0.07 ± 0.01	0.02 ± 0.01	0.04 ± 0.04	0.03 ± 0.01
Blood	3.17 ± 0.45	0.12 ± 0.11	0.01 ± 0.01	0.02 ± 0.01	1.28 ± 0.09	0.16 ± 0.05	0.14 ± 0.06	0.01 ± 0.01
Heart	1.35 ± 0.26	0.24 ± 0.12	0.01 ± 0.02	0.01 ± 0.01	0.66 ± 0.17	0.06 ± 0.04	0.06 ± 0.04	0.06 ± 0.02
Lung	2.97 ± 0.71	0.28 ± 0.07	0.13 ± 0.10	0.07 ± 0.05	1.31 ± 0.29	0.31 ± 0.14	0.20 ± 0.04	0.12 ± 0.05
Liver	1.41 ± 0.22	0.57 ± 0.09	0.60 ± 0.03	0.60 ± 0.10	0.67 ± 0.17	0.50 ± 0.12	0.36 ± 0.03	0.26 ± 0.01
Spleen	0.93 ± 0.37	0.17 ± 0.06	0.15 ± 0.10	0.12 ± 0.13	0.54 ± 0.13	0.24 ± 0.11	0.19 ± 0.10	0.14 ± 0.01
Stomach	2.18 ± 0.28	1.30 ± 0.12	1.14 ± 0.13	1.17 ± 0.48	0.95 ± 0.15	0.28 ± 0.03	0.49 ± 0.14	0.41 ± 0.01
Kidney	15.19 ± 2.75	6.84 ± 0.92	6.82 ± 1.19	5.44 ± 1.58	9.06 ± 2.20*	5.54 ± 0.63*	6.25 ± 0.51	4.21 ± 0.03
Muscle	0.37 ± 0.26	0.01 ± 0.01	0.02 ± 0.02	0.02 ± 0.01	0.32 ± 0.09	0.06 ± 0.03	0.11 ± 0.05	0.09 ± 0.01
Pancreas	0.99 ± 0.27	0.23 ± 0.12	0.14 ± 0.06	0.10 ± 0.08	0.40 ± 0.08	0.12 ± 0.10	0.13 ± 0.08	0.15 ± 0.04
Bone	0.59 ± 0.39	0.10 ± 0.09	0.10 ± 0.08	0.04 ± 0.04	0.13 ± 0.10	0.08 ± 0.05	0.02 ± 0.01	0.06 ± 0.01
Skin	2.16 ± 1.28	0.27 ± 0.12	0.27 ± 0.28	0.26 ± 0.08	1.63 ± 0.43	0.37 ± 0.11	0.12 ± 0.10	0.16 ± 0.13
%ID								
Intestine	1.65 ± 0.26	1.30 ± 0.32	0.97 ± 0.38	0.74 ± 0.13	0.95 ± 0.14	0.68 ± 0.26	1.45 ± 0.85	0.76 ± 0.45
Urine	60.80 ± 4.05	88.46 ± 1.75	88.39 ± 3.06	93.23 ± 1.60	83.56 ± 0.49	89.65 ± 6.24	91.38 ± 1.85	93.57 ± 0.12
Uptake ratio [†]								
Tumor/blood	5.80	158.75	1,860.00	338.50	9.18	56.19	37.86	440.00
Tumor/kidneys	1.21	2.79	2.73	1.24	1.30	1.62	0.85	1.05
Tumor/lung	6.19	68.04	143.08	96.71	8.97	29.00	26.50	36.67
Tumor/liver	13.04	33.42	31.00	11.28	17.54	17.98	14.72	16.92
Tumor/muscle	49.70	1905.00	930.00	338.50	36.72	149.83	48.18	48.89
Tumor/skin	8.51	70.56	68.89	26.04	7.21	24.30	44.17	27.50

**P* < 0.05 for determining significance of differences in tumor and kidney uptake between ¹¹¹In-DOTA-GGNle-CycMSH_{hex} and ¹¹¹In-DOTA-GENle-CycMSH_{hex}.
[†]Tumor to normal tissue.
Data are %ID/g or %ID (mean ± SD, *n* = 5).

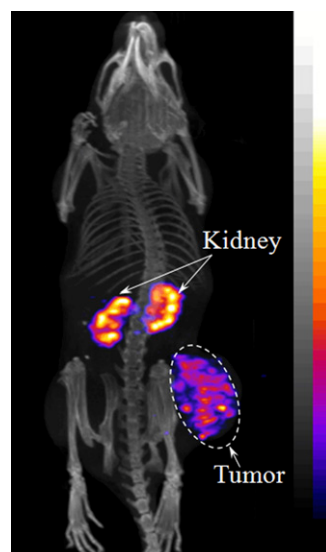
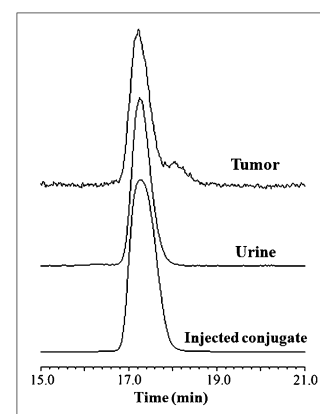


FIGURE 3. Representative whole-body SPECT/CT image of B16/F1 melanoma-bearing mouse (10 d after cell inoculation) 2 h after injection of 14.8 MBq of ^{111}In -DOTA-GGNle-CycMSH_{hex}.

observed in the difference in melanoma uptake between ^{111}In -DOTA-GGNle-CycMSH_{hex} and ^{111}In -DOTA-GENle-CycMSH_{hex} in B16/F1 melanoma-bearing C57 mice. Tumor uptake of ^{111}In -DOTA-GGNle-CycMSH_{hex} was 2, 2.5, and 3 times that of ^{111}In -DOTA-GENle-CycMSH_{hex} at 0.5, 2, and 4 h after injection, respectively (Table 2). In our previous report, the introduction of a negatively charged -GE- linker resulted in 44% reduced kidney uptake of ^{111}In -DOTA-GE-CycMSH at 4 h after injection, compared with ^{111}In -DOTA-CycMSH (15). In this study, kidney uptake for ^{111}In -DOTA-GENle-CycMSH_{hex} was 40% lower than that for ^{111}In -DOTA-GGNle-CycMSH_{hex} at 0.5 h after injection ($P < 0.05$) (Table 2).

Presently, the lactam bridge-cyclized ^{111}In -DOTA-Nle-CycMSH_{hex} and the metal-cyclized ^{111}In -DOTA-Re(Arg¹¹)CCMSH have displayed the highest comparable melanoma uptake among all reported ^{111}In -labeled linear and cyclic α -MSH peptides (13,19). The respective values for melanoma uptake were 17.29 ± 2.49 and 17.41 ± 5.63 %ID/g at 2 and 4 h after injection for ^{111}In -DOTA-Re(Arg¹¹)CCMSH (13) and 19.39 ± 1.65 and 17.01 ± 2.54 %ID/g at 2 and 4 h after injection for ^{111}In -DOTA-Nle-CycMSH_{hex} (19). Meanwhile, ^{111}In -DOTA-Nle-CycMSH_{hex} showed ratios of tumor-to-kidney uptake that were similar to those for ^{111}In -DOTA-Re(Arg¹¹)CCMSH at 2 and 24 h after injection (19). In this study, the introduction of the -GG- linker maintained high melanoma uptake of ^{111}In -DOTA-GGNle-CycMSH_{hex} (19.05 ± 5.04 and 18.6 ± 3.56 %ID/g at 2 and 4 h after injection, respectively), compared with ^{111}In -DOTA-Nle-CycMSH_{hex}, as was consistent with their similar MC1 receptor-binding affinities (2.1 nM vs. 1.8 nM). Interestingly, the introduction of the -GG- linker reduced liver and kidney uptake of ^{111}In -DOTA-GGNle-CycMSH_{hex}, compared with ^{111}In -DOTA-Nle-CycMSH_{hex} (19). The reduction in liver and kidney uptake might be attributed to the relatively faster whole-body clearance of ^{111}In -DOTA-GGNle-CycMSH_{hex}. Approximately 88% of ^{111}In -DOTA-GGNle-CycMSH_{hex}

FIGURE 4. Radioactive HPLC profiles of ^{111}In -DOTA-GGNle-CycMSH_{hex} (injected conjugate) and its metabolites in urine and tumor 2 h after injection.



activity cleared from the body via the urinary system at 2 h after injection, whereas 82% of ^{111}In -DOTA-Nle-CycMSH_{hex} activity washed out of the body via the urinary tract at 2 h after injection (19). ^{111}In -DOTA-GGNle-CycMSH_{hex} exhibited 61%, 65%, and 68% less liver uptake than ^{111}In -DOTA-Nle-CycMSH_{hex} (Fig. 5) and 28%, 32%, and 42% less kidney uptake than ^{111}In -DOTA-Nle-CycMSH_{hex} at 2, 4, and 24 h after injection, respectively (Fig. 5). The maintained high melanoma uptake coupled with the decreased liver and kidney uptake resulted in enhanced ratios of tumor-to-liver and tumor-to-kidney uptake for ^{111}In -DOTA-GGNle-CycMSH_{hex}, compared with ^{111}In -DOTA-Nle-CycMSH_{hex}, at 2 and 4 h after injection (Fig. 6). The tumor-to-liver ratios of ^{111}In -DOTA-GGNle-CycMSH_{hex} were 2.5 and 3.1 times those of ^{111}In -DOTA-Nle-CycMSH_{hex} at 2 and 4 h after injection, whereas the tumor-to-kidney ratios of ^{111}In -DOTA-GGNle-CycMSH_{hex} were 1.4 and 1.6 times those of ^{111}In -DOTA-Nle-CycMSH_{hex} at 2 and 4 h after injection.

As shown in Figure 3, the enhanced tumor-to-liver and tumor-to-kidney ratios of ^{111}In -DOTA-GGNle-CycMSH_{hex} generated high contrast between tumor and background. The flank melanoma lesions were clearly visualized by SPECT/CT using ^{111}In -DOTA-GGNle-CycMSH_{hex} as an imaging probe, highlighting its potential as an effective imaging agent for melanoma detection. ^{111}In -DOTA-GGNle-CycMSH_{hex} maintained intact in melanoma and urine at 2 h after injection (Fig. 4). From the therapeutic point of view, the enhanced tumor-to-liver and tumor-to-kidney ratios of ^{111}In -DOTA-GGNle-CycMSH_{hex} would decrease the absorbed doses to the liver and kidneys when the therapeutic radionuclide-labeled DOTA-GGNle-CycMSH_{hex} is used for melanoma treatment. In other words, the improvement in tumor-to-liver and tumor-to-kidney ratios would potentially increase the absorbed dose to the tumor while keeping the liver and kidneys safe when melanoma is treated with therapeutic radionuclide-labeled DOTA-GGNle-CycMSH_{hex}.

CONCLUSION

The amino acid linkers exhibited profound effects on the melanoma-targeting and pharmacokinetic properties of the

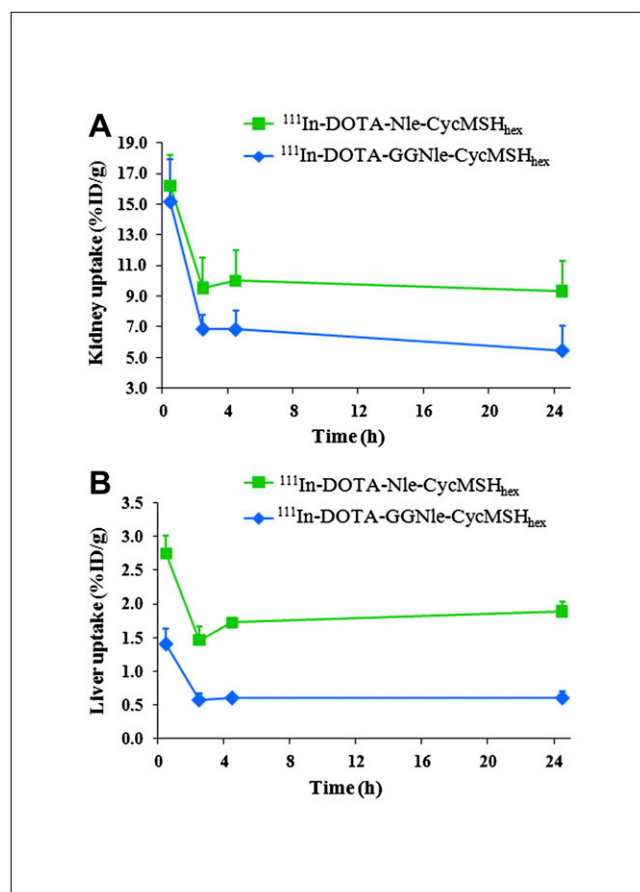


FIGURE 5. Kidney (A) and liver (B) uptake of ^{111}In -DOTA-Nle-CycMSH_{hex} and ^{111}In -DOTA-GGNle-CycMSH_{hex}. Data of ^{111}In -DOTA-Nle-CycMSH_{hex} were cited from reference 19 for comparison.

^{111}In -labeled lactam bridge-cyclized α -MSH peptides. Introduction of the -GG- linker maintained high melanoma uptake while reducing kidney and liver uptake of ^{111}In -DOTA-GGNle-CycMSH_{hex}, highlighting its potential as an effective imaging probe for melanoma detection and as a therapeutic peptide for melanoma treatment when labeled with a therapeutic radionuclide.

DISCLOSURE STATEMENT

The costs of publication of this article were defrayed in part by the payment of page charges. Therefore, and solely to indicate this fact, this article is hereby marked “advertisement” in accordance with 18 USC section 1734.

ACKNOWLEDGMENTS

This work was supported in part by NIH grant NM-INBRE P20RR016480 and the University of New Mexico STC Gap Fund. Figure 3 was generated by the Keck-UNM Small Animal Imaging Resource established with funding from the W.M. Keck Foundation and the University of New Mexico Cancer Research and Treatment Center (NIH P30 CA118100).

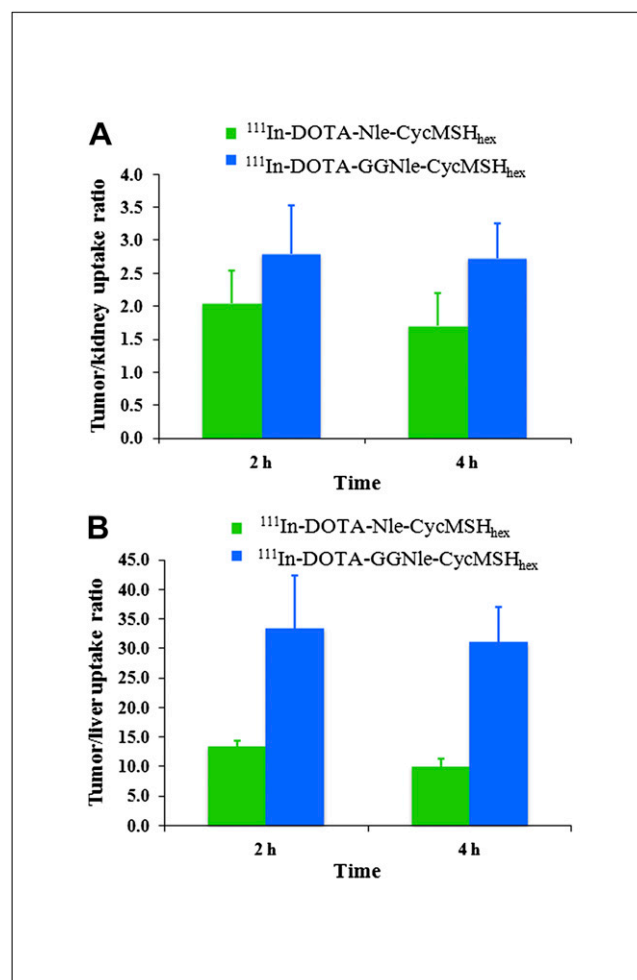


FIGURE 6. Tumor-to-kidney (A) and tumor-to-liver (B) ratios of ^{111}In -DOTA-Nle-CycMSH_{hex} and ^{111}In -DOTA-GGNle-CycMSH_{hex} 2 and 4 h after injection. Data of ^{111}In -DOTA-Nle-CycMSH_{hex} were cited from reference 19 for comparison.

REFERENCES

1. Siegrist W, Solca F, Stutz S, et al. Characterization of receptors for alpha-melanocyte-stimulating hormone on human melanoma cells. *Cancer Res.* 1989;49:6352–6358.
2. Tatro JB, Reichlin S. Specific receptors for alpha-melanocyte-stimulating hormone are widely distributed in tissues of rodents. *Endocrinology.* 1987;121:1900–1907.
3. Miao Y, Whitener D, Feng W, Owen NK, Chen J, Quinn TP. Evaluation of the human melanoma targeting properties of radiolabeled alpha-melanocyte stimulating hormone peptide analogues. *Bioconjug Chem.* 2003;14:1177–1184.
4. Miao Y, Owen NK, Whitener D, Gallazzi F, Hoffman TJ, Quinn TP. In vivo evaluation of ^{188}Re -labeled alpha-melanocyte stimulating hormone peptide analogs for melanoma therapy. *Int J Cancer.* 2002;101:480–487.
5. Chen J, Cheng Z, Hoffman TJ, Jurisson SS, Quinn TP. Melanoma-targeting properties of ^{99m}Tc -labeled cyclic alpha-melanocyte-stimulating hormone peptide analogues. *Cancer Res.* 2000;60:5649–5658.
6. Froidevaux S, Calame-Christe M, Tanner H, Eberle AN. Melanoma targeting with DOTA-alpha-melanocyte-stimulating hormone analogs: structural parameters affecting tumor uptake and kidney uptake. *J Nucl Med.* 2005;46:887–895.
7. Froidevaux S, Calame-Christe M, Schuhmacher J, et al. A gallium-labeled DOTA-alpha-melanocyte-stimulating hormone analog for PET imaging of melanoma metastases. *J Nucl Med.* 2004;45:116–123.
8. Froidevaux S, Calame-Christe M, Tanner H, Sumanovski L, Eberle AN. A novel DOTA-alpha-melanocyte-stimulating hormone analog for metastatic melanoma diagnosis. *J Nucl Med.* 2002;43:1699–1706.

9. Miao Y, Owen NK, Fisher DR, Hoffman TJ, Quinn TP. Therapeutic efficacy of a ^{188}Re -labeled alpha-melanocyte-stimulating hormone peptide analog in murine and human melanoma-bearing mouse models. *J Nucl Med.* 2005;46:121–129.
10. Miao Y, Hylarides M, Fisher DR, et al. Melanoma therapy via peptide-targeted alpha-radiation. *Clin Cancer Res.* 2005;11:5616–5621.
11. Wei L, Butcher C, Miao Y, et al. Synthesis and biologic evaluation of ^{64}Cu -labeled rhenium-cyclized alpha-MSH peptide analog using a cross-bridged cyclam chelator. *J Nucl Med.* 2007;48:64–72.
12. Miao Y, Benwell K, Quinn TP. $^{99\text{m}}\text{Tc}$ - and ^{111}In -labeled alpha-melanocyte-stimulating hormone peptides as imaging probes for primary and pulmonary metastatic melanoma detection. *J Nucl Med.* 2007;48:73–80.
13. Cheng Z, Chen J, Miao Y, Owen NK, Quinn TP, Jurisson SS. Modification of the structure of a metalloprotein: synthesis and biological evaluation of ^{111}In -labeled DOTA-conjugated rhenium-cyclized alpha-MSH analogues. *J Med Chem.* 2002;45:3048–3056.
14. Cheng Z, Xiong Z, Subbarayan M, Chen X, Gambhir SS. ^{64}Cu -labeled alpha-melanocyte-stimulating hormone analog for MicroPET imaging of melanocortin 1 receptor expression. *Bioconjug Chem.* 2007;18:765–772.
15. Miao Y, Gallazzi F, Guo H, Quinn TP. ^{111}In -labeled lactam bridge-cyclized alpha-melanocyte stimulating hormone peptide analogues for melanoma imaging. *Bioconjug Chem.* 2008;19:539–547.
16. Guo H, Shenoy N, Gershman BM, Yang J, Sklar LA, Miao Y. Metastatic melanoma imaging with an ^{111}In -labeled lactam bridge-cyclized alpha-melanocyte-stimulating hormone peptide. *Nucl Med Biol.* 2009;36:267–276.
17. Guo H, Yang J, Gallazzi F, Prossnitz ER, Sklar LA, Miao Y. Effect of DOTA position on melanoma targeting and pharmacokinetic properties of ^{111}In -labeled lactam bridge-cyclized α -melanocyte stimulating hormone peptide. *Bioconjug Chem.* 2009;20:2162–2168.
18. Guo H, Yang J, Shenoy N, Miao Y. Gallium-67-labeled lactam bridge-cyclized alpha-melanocyte stimulating hormone peptide for primary and metastatic melanoma imaging. *Bioconjug Chem.* 2009;20:2356–2363.
19. Guo H, Yang J, Gallazzi F, Miao Y. Reduction of the ring size of radiolabeled lactam bridge-cyclized alpha-MSH peptide resulting in enhanced melanoma uptake. *J Nucl Med.* 2010;51:418–426.
20. Chen J, Cheng Z, Owen NK, et al. Evaluation of an ^{111}In -DOTA-rhenium cyclized α -MSH analog: a novel cyclic-peptide analog with improved tumor-targeting properties. *J Nucl Med.* 2001;42:1847–1855.
21. Hoffman TJ, Gali H, Smith CJ, et al. Novel series of ^{111}In -labeled bombesin analogs as potential radiopharmaceuticals for specific targeting of gastrin-releasing peptide receptors expressed on human prostate cancer cells. *J Nucl Med.* 2003;44:823–831.
22. Garcia Garayoa E, Schweinsberg C, Maes V, et al. Influence of the molecular charge on the biodistribution of bombesin analogues labeled with the $^{99\text{m}}\text{Tc}(\text{CO})_3$ -core. *Bioconjug Chem.* 2008;19:2409–2416.
23. Fragogeorgi EA, Zikos C, Gourni E, et al. Spacer site modifications for the improvement of the *in vitro* and *in vivo* binding properties of $^{99\text{m}}\text{Tc}$ -N₃S-X-bombesin[2–14] derivatives. *Bioconjug Chem.* 2009;20:856–867.
24. Garrison JC, Rold TL, Sieckman GL, et al. Evaluation of the pharmacokinetic effects of various linking group using the ^{111}In -DOTA-X-BBN(7–14)NH₂ structural paradigm in a prostate cancer model. *Bioconjug Chem.* 2008;19:1803–1812.
25. Parry JJ, Kelly TS, Andrews R, Rogers BE. *In vitro* and *in vivo* evaluation of ^{64}Cu -labeled DOTA-linker-bombesin(7–14) analogues containing different amino acid linker moieties. *Bioconjug Chem.* 2007;18:1110–1117.
26. Liu S, He Z, Hsieh WY, Kim YS, Jiang Y. Impact of PKM linkers on biodistribution characteristics of the $^{99\text{m}}\text{Tc}$ -labeled cyclic RGDfK dimer. *Bioconjug Chem.* 2006;17:1499–1507.
27. Shi J, Wang L, Kim YS, et al. Improving tumor uptake and excretion kinetics of $^{99\text{m}}\text{Tc}$ -labeled cyclic arginine-glycine-aspartic (RGD) dimers with triglycine linkers. *J Med Chem.* 2008;51:7980–7990.
28. Wang L, Shi J, Kim YS, et al. Improving tumor-targeting capability and pharmacokinetics of $^{99\text{m}}\text{Tc}$ -labeled cyclic RGD dimers with PEG₄ linkers. *Mol Pharm.* 2009;6:231–245.
29. Shi J, Kim YS, Zhai S, Liu Z, Chen X, Liu S. Improving tumor uptake and pharmacokinetics of ^{64}Cu -labeled cyclic RGD peptide dimers with Gly₃ and PEG₄ linkers. *Bioconjug Chem.* 2009;20:750–759.



The Journal of
NUCLEAR MEDICINE

Effects of the Amino Acid Linkers on the Melanoma-Targeting and Pharmacokinetic Properties of ^{111}In -Labeled Lactam Bridge-Cyclized α -MSH Peptides

Haixun Guo, Jianquan Yang, Fabio Gallazzi and Yubin Miao

J Nucl Med. 2011;52:608-616.

Published online: March 18, 2011.

Doi: 10.2967/jnumed.110.086009

This article and updated information are available at:

<http://jnm.snmjournals.org/content/52/4/608>

Information about reproducing figures, tables, or other portions of this article can be found online at:

<http://jnm.snmjournals.org/site/misc/permission.xhtml>

Information about subscriptions to JNM can be found at:

<http://jnm.snmjournals.org/site/subscriptions/online.xhtml>

The Journal of Nuclear Medicine is published monthly.
SNMMI | Society of Nuclear Medicine and Molecular Imaging
1850 Samuel Morse Drive, Reston, VA 20190.
(Print ISSN: 0161-5505, Online ISSN: 2159-662X)

© Copyright 2011 SNMMI; all rights reserved.

 SOCIETY OF
NUCLEAR MEDICINE
AND MOLECULAR IMAGING